A BULK PZT MICROSENSOR FOR IN-SITU TISSUE CONTRAST DETECTION DURING FINE NEEDLE ASPIRATION BIOPSY OF THYROID NODULES

Tao Li[*1], Roma Y. Gianchandani[2] and Yogesh B. Gianchandani[1]
[1]*Engineering Research Center for Wireless Integrated Microsystems*
[2]*Department of Internal Medicine, Division of Metabolism, Endocrinology & Diabetes*
University of Michigan, Ann Arbor, MI, USA

ABSTRACT

This paper describes a piezoelectric sensor integrated into a cavity at the tip of a biopsy needle intended for fine needle aspiration (FNA) of thyroid nodules. Located on a steel diaphragm of 300 μm radius and 23 μm average thickness, it is intended to aid in tissue differentiation, providing information that is complementary to any imaging method that may be used concurrently. The sensor is fabricated from bulk lead zirconate titanate (PZT) using a customized process. Micro electro-discharge machining is used to form a steel tool that is subsequently used for batch-mode ultrasonic machining of bulk PZT ceramic. The resulting sensor is 50 μm thick and 200 μm in diameter. Devices were tested in materials that mimic the texture of human tissue in the training of physicians, and were separately tested with porcine fat and muscle tissue. The magnitude and frequency of a resonant peak shows tissue-specific characteristics as the needle is inserted into tissue. For example, in the porcine tissue sample, the magnitude and peak frequency respectively change from ≈2118 Ω and ≈163 MHz to ≈562 Ω and ≈150 MHz as the needle moves from fat to muscle tissue.

I. INTRODUCTION

While thyroid cancer results in <1% of cancer deaths, its clinical diagnosis can be very challenging. This is because malignant tumors must be differentiated from benign nodules. Since thyroid nodules can be observed in about 20% of the general US population [1], and the ultrasound characteristics of benign and malignant nodules are similar, fine needle aspiration (FNA) biopsy is usually required to make a final diagnosis. This is typically performed with a (20-27 gauge) needle attached to a 10 mL syringe for suction of thyroid tissue, which is then examined by a cytologist.

The biopsy is challenging in itself because of the precision required in recovering a sample from the small target volumes. To aid this, conventional ultrasound imaging is performed in real time, especially for those nodules that are difficult to palpate or contain complicated solid and cystic areas. This adds significant complexity, requiring special training and equipment that only limited hospitals can afford, yet is not always effective. At least 2-5% of FNAs are read as non-diagnostic because of improper sampling [1-3]. A biopsy needle that can detect different tissue planes or variations of densities (e.g., solid vs. cystic) can make the detection of this easily cured cancer not only more accurate, but more widely accessible.

This paper describes a piezoelectric sensor integrated into a cavity at the tip of a biopsy needle intended for fine needle aspiration (FNA) of thyroid nodules (Fig. 1). The sensor is fabricated from bulk lead zirconate titanate (PZT) using a customized process. Micro electro-discharge machining (μEDM) is used to form a steel tool that is subsequently used for batch-mode micro ultrasonic machining (μUSM) of bulk PZT ceramic. The devices are tested in materials that mimic the texture of human tissue in the training of physicians, and were separately tested with porcine fat and muscle tissue.

II. DESIGN & FABRICATION

Piezoelectric materials such as piezoelectric ceramics (PZT series, etc.), polymers (PVDF, etc.), quartz, and ZnO, have been widely used in the fabrication of sensors and actuators [4,5]. PZT is of particular interest for MEMS applications due to its high piezoelectric coefficients and good electro-mechanical coupling. When the mechanical boundary condition of a PZT-horn assembly changes by touching different types of rock materials, the resonance frequency and the electric impedance of the assembly change accordingly [6].

The scheme for *in-situ* detection of tissue contrast during thyroid biopsy is shown in Fig. 1. A PZT sensor is mounted at the tip of the needle that is connected to a spectrum analyzer for real-time impedance measurement. Figure 2 shows the schematics of the proposed device. The PZT disc is located against a diaphragm and within a cavity micromachined into the wall of the needle, which also serves as a ground plane for one electrode. The second lead, which is to the top of the PZT disc, is a flexible insulated wire that extends along the lumen of the needle. Since the

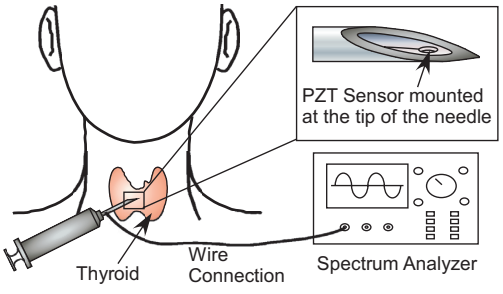

Fig. 1: Schematic system diagram of the proposed tissue contrast sensor used for thyroid biopsy.

[*] *Corresponding author:* 1301 Beal Ave., Ann Arbor, MI, 48109, USA; Tel: (734) 647-2040, Fax: (734) 763-9324. E-mail: litz@umich.edu

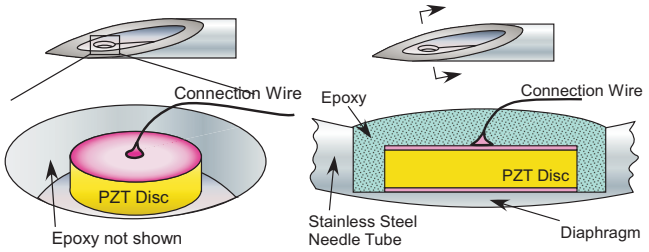

(a) (b)

Fig. 2: Schematics of the tissue contrast sensor. (a) Perspective view with sealing epoxy removed; (b) Cross sectional view.

diaphragm makes contact with the tissues encountered during a biopsy procedure, and the tissue types have different acousto-mechanical impedance, the vibration characteristics of the diaphragm and the PZT disc will change accordingly. This change in mechanical resonance is transduced to a change in electric impedance of the PZT disc by the piezoelectric effect and can be detected by the impedance spectrum analyzer. Thus, the changes in the electric impedance provide a measure of tissue contrast in this preliminary version of the sensor.

The fabrication process for the PZT disc is shown in Fig. 3a. A bulk PZT-5H plate, which has superior material properties for sensor applications, was bonded to a glass substrate by a polymer. The SEDUS process [7] was carried out to transfer a disc-array pattern onto the PZT plate. This is a batch-mode micromachining process that uses ultrasonic machining with the help of electro-discharge machined steel tools, and results in the devices shown in Fig. 4. The discs were released by lapping away the extra thickness of the PZT plate. They have diameter of 200 μm and thickness of 50 μm. The interior apex of the biopsy needle was then also machined by electro-discharge machining to form the cavity, and the PZT was integrated as illustrated in Fig. 3b. The cavity diameter and depth are 300 μm and 150 μm, respectively. This results in a diaphragm with varying thickness of 10-36 μm on the 20-gauge needle.

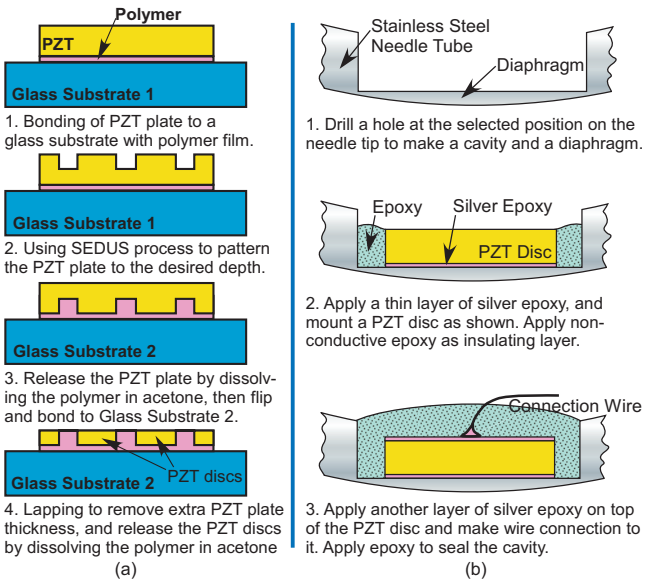

(a) (b)

Fig. 3: Diagram of fabrication process flow for: (a) PZT disc; (b) the in-situ tissue contrast sensor at the tip of a 20G syringe needle.

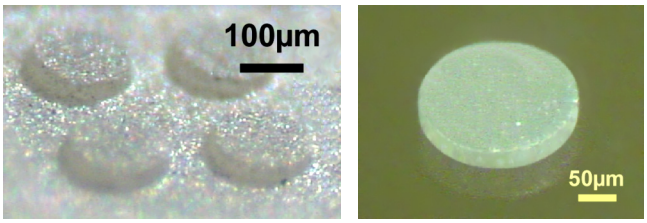

(a) (b)

Fig. 4: Photos of: (a) PZT disc array batch fabricated by SEDUS process using batch µUSM to transfer a pattern defined by serial µEDM. (b) Released PZT disc. Diameter: 200 µm. Thickness: 50 µm.

A thin layer of silver conductive epoxy was used to attach the PZT disc to the bottom of the cavity, as well as to attach the lead wire to the top surface of the disc. Non-conductive epoxy was used as insulating layer and sealing material. Figure 5 shows the micromachined cavity before sensor placement, whereas Fig. 6 shows the finished device.

III. EXPERIMENTAL RESULTS

Figure 7 illustrates the procedure used for physician training in thyroid FNA biopsy: a pickled olive simulates the thyroid nodule, while an Aquaflex® ultrasound gel pad (Model 04-02 from Parker Labs Inc.) and dampened sponge simulate the surrounding tissues. A trainee holds the ultrasound probe with one hand and inserts the needle into the target region (Fig. 7b) while observing its position using a real-time 2D ultrasound image (Fig. 7c).

The fabricated devices were tested by penetrating the biopsy needle into: (A) the physician training arrangement of Fig. 7a; and (B) porcine tissue consisting of fat and muscle layers. An HP4195 spectrum analyzer was used to

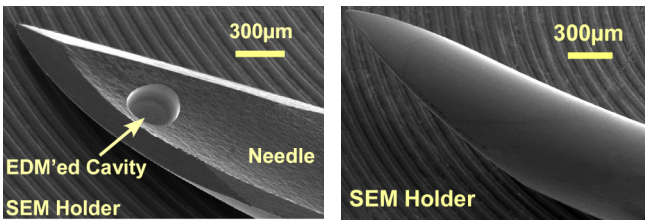

(a) (b)

Fig. 5: SEM photos of µEDM'ed syringe needle tip with the cavity for mounting PZT sensor: (a) inner side view; (b) outer side view.

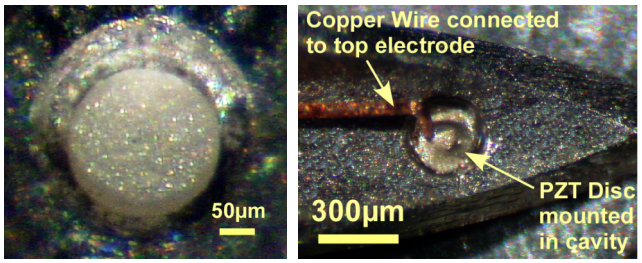

(a) (b)

Fig. 6: Photos of: (a) A PZT disc mounted in the cavity at the tip of a syringe needle. Cavity diameter: 300 µm, depth: 150 µm. Corresponding diaphragm thickness: max. 36 µm, min. 10 µm; (b) Finished device before sealing epoxy is applied. Coated copper wire is used to make connection to the top electrode of the PZT disc. The stainless steel needle body is used as ground.

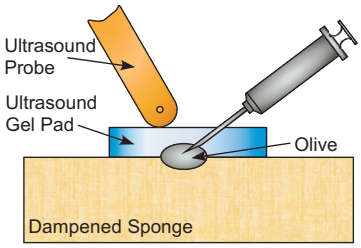

(a)

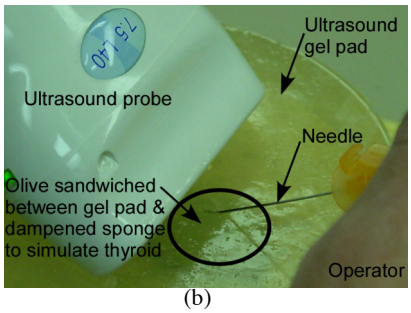

(b)

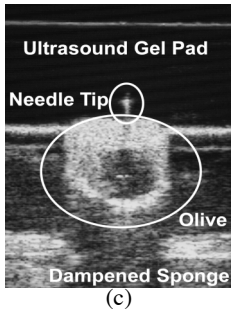

(c)

Fig. 7: Physician training for thyroid biopsy. (a) Schematics showing test setup and tissue model. (b) Photo of operation. Medical ultrasound probe is used to guide the process, the image of which is shown in (c).

obtain impedance spectra.

The results of test A are shown in Fig. 8 and Fig. 9. A resonance mode with a relatively high frequency and large Q was selected for testing. When the needle was inserted from free space into the ultrasound gel pad, the resonance frequency dropped from 176 MHz to 154 MHz. Both the resonance frequency and the peak impedance decreased gradually with advancement of the needle into the gel pad. After the needle tip reached the olive, the resonance frequency stayed almost constant while the impedance peak magnitude started increasing with injecting depth into the olive. The electrical characteristics are thereby indicative of a tissue contrast between the olive and the ultrasound gel pad, which respectively emulate a thyroid nodule and the surrounding tissues.

The results of test B are shown in Fig. 10. Both the resonance frequency and the impedance peak magnitude gradually decrease as the needle is inserted into the fatty tissue. Once the needle tip moves into the muscle, the impedance peak magnitude starts to increase slightly, while the resonance frequency further drops with a much smaller slope (≈1/5 of that in fat).

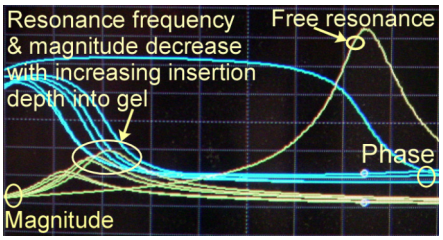

(a)

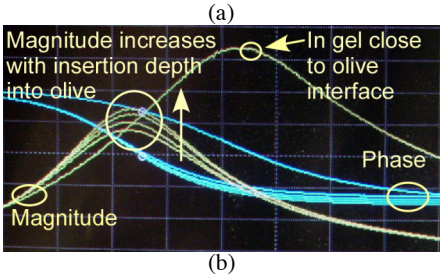

(b)

Fig. 8: Screen prints of HP 4195 Spectrum Analyzer used to measure the impedance of the PZT disc vs. frequency sweep. (a) Needle tip inserted from free space into the ultrasound gel pad. (b) Needle tip inserted from the gel pad into the olive.

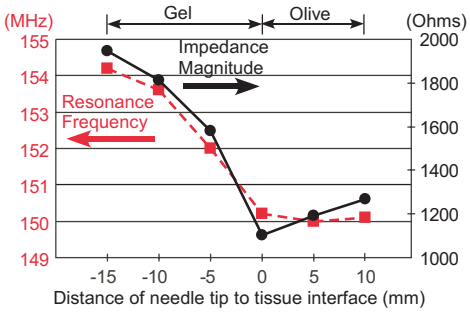

Fig. 9: Measured resonance frequency and peak magnitude of the impedance of the PZT sensor vs. proximity to tissue interface. It shows that once the tip moves into the olive, the resonance frequency remains constant while the impedance peak magnitude starts increasing.

The porcine fat is not optically transparent like the ultrasound gel pad, making visual observation of the needle position more difficult for test B. Two additional tests were then carried out to individually study the response of the sensor to porcine fat or muscle by inserting the needle directly from free space into each kind of tissue. As shown in Fig. 11, impedance characteristics similar to that in Fig. 10 were observed in each case. This confirms that the electrical characteristics shown in Fig. 10 demonstrated the tissue contrast between animal fat and muscle.

IV. PRELIMINARY ANALYSIS

A circuit model for the biopsy tissue contrast sensor is shown in Fig. 12. A lumped-parameter Butterworth-Van Dyke (BVD) equivalent circuit can be used to represent the PZT disc [8], and the stainless steel needle tube along with the inside copper wire is modeled using transmission line characteristics. The motional arm (L_1, R_1 and C_1) of the BVD circuit is coupled with the diaphragm and surrounding tissue by the piezoelectric effect. The PZT disk has a thickness of t=50 μm, and the sound velocity in the PZT material is c≈3319 m/s. This results in the first thickness-mode free mechanical resonance frequency of ≈33 MHz

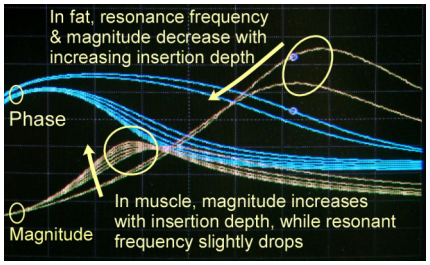

(a)

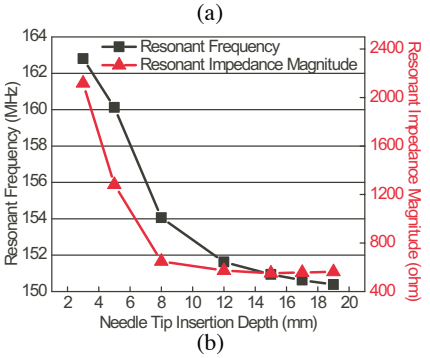

(b)

Fig. 10: (a) Screen image of HP4195 showing resonant impedance change when needle tip goes from porcine fat layer to muscle layer. (b) Measured resonance frequency and peak magnitude of the PZT impedance vs. needle insertion depth into the animal tissue.

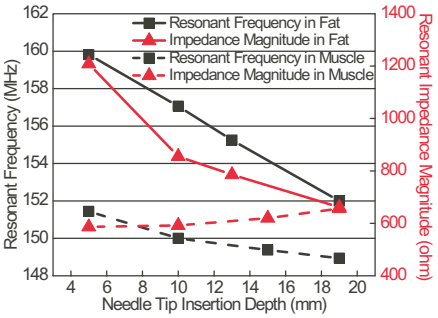

Fig. 11: Measured resonance frequency and peak magnitude of the impedance of the PZT sensor vs. needle tip insertion depth from free space directly into fat or muscle.

when $t=\lambda/2$, where λ is the sound wavelength in the material [9]. The resonance frequency used for measurement (≈170 MHz) is around the 5th harmonic resonance, and is also coupled with the transmission line characteristics of the needle tube, as well as the mechanical characteristics of the diaphragm and tissue.

The coupled transmission line characteristic of the needle tube is not directly needed to detect a contrast in the tissue. However, it is helpful in estimating the attenuation of the stimulating and sensed signals. A transmission line analysis was performed by using the coaxial line model and replacing the PZT disc with an equivalent static capacitor. The extension wire that connects the needle tube to the impedance analyzer was neglected for this analysis as it was compensated during measurement. According to the analysis, the input impedance Z_{in} of this model smoothly drops within the frequency range of interest (Fig. 13a), and the length of the equivalent coaxial cable can be considered much shorter than the transmission line characteristic wavelength. The ratio of the power delivered to the PZT disc through the needle tube and copper wire is ≈65% at ≈160 MHz (Fig. 13b). A more detailed analysis of the PZT sensor characteristics will be pursued in later efforts.

V. CONCLUSIONS

A micromachined device has been demonstrated to achieve *in-situ* real-time tissue contrast detection during FNA biopsy of thyroid nodules. A batch-fabricated bulk PZT sensor was implemented into a cavity that is in the wall of a needle at its apex. The device was tested in a simulated scheme for physician training, as well as in porcine tissue consisting of fat and muscle layers. The device demonstrated tissue contrast in both of the test schemes through a change in the resonance frequency and peak magnitude of the PZT electric impedance. A preliminary analysis based on a circuit model has been carried out for the tissue contrast sensor. The experimental results are very promising for further improvements, and will be pursued in future efforts.

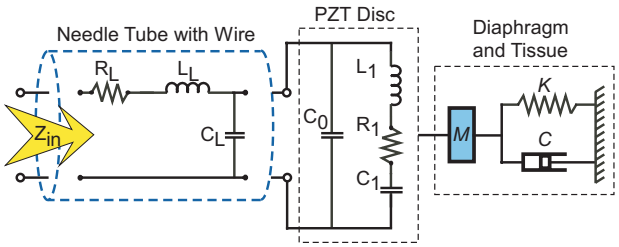

Fig. 12: A circuit model for the biopsy tissue contrast sensor.

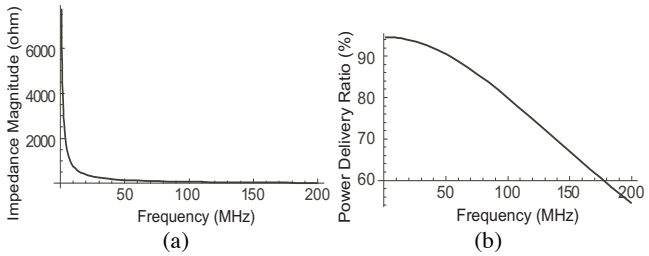

Fig. 13: A transmission line analysis carried out to evaluate the effect of the needle tube and the inside copper wire on the measured impedance characteristics. Coaxial line model was used and the PZT disc was replaced by an equivalent static capacitor. (a) Input impedance Z_{in} vs. frequency. (b) Ratio of power delivered to the PZT disc vs. frequency.

ACKNOWLEDGEMENT

The authors are grateful to the Solid-State Electronics Laboratory (SSEL) colleagues at the University of Michigan for their help with equipment. This work was supported primarily by the Engineering Research Centers Program of the National Science Foundation under Award Number EEC-9986866. Facilities used for this research include the Solid-State Electronics Laboratory (SSEL) at the University of Michigan.

REFERENCES

[1] F. Pacini, L.J. De Groot, "Thyroid Neoplasia," *The Thyroid and its Diseases*, 6th ed., W.B. Saunders Company, 1996, updated online at http://www.thyroidmanager.org, May 2004

[2] S. Takashima, H. Fukuda, T. Kobayashi, "Thyroid nodules: clinical effect of ultrasound-guided fine-needle aspiration biopsy," *J. Clin. Ultrasound*, 22(9), pp. 535-42, Nov.-Dec. 1994

[3] H. Gharib, J.R. Goellner, "Fine-needle aspiration biopsy of the thyroid: an appraisal," *Ann. Intern. Med.* 118(4), pp.282-9, Feb. 1993

[4] H. Zhang, E.S. Kim, "Micromachined acoustic resonant mass sensor," *IEEE/ASME J. Microelectromechanical Systems,* 14(4), pp. 699-706, Aug. 2000

[5] G.-H. Feng, C.C. Sharp, Q.F. Zhou, W. Pang, E.S. Kim, K.K. Shung, "Fabrication of MEMS ZnO dome-shaped-diaphragm transducers for high frequency ultrasonic imaging," *J. Micromechanics and Microengineering,* 15(3), pp. 586-590, 2005

[6] Z. Chang, S. Sherrit, X. Bao, Y. Bar-Cohen, "In-situ rock probing using the ultrasonic/sonic driller/corer," *Proc. SPIE Smart Structures Conference*, San Diego, Mar. 2003

[7] T. Li, Y.B. Gianchandani, "A die-scale micromachining process for bulk PZT and its application to in-plane actuators," *Proc. IEEE MEMS 2005*, pp. 387-390, Jan. 2005

[8] *IEEE Standard on Piezoelectricity*, ANSI/IEEE Std. 176-1987, withdrawn in 2000

[9] T. Ikeda, *Fundamentals of Piezoelectricity*, Oxford University Press, New York, 1990